

Reinforcing Thermosets Using Crystalline Desoxyanisoin Structures

Polina R. Ware, Alan J. Lesser

Department of Polymer Science and Engineering, University of Massachusetts, Amherst, Massachusetts 01003

Correspondence to: A. J. Lesser (ajl@polysci.umass.edu)

ABSTRACT: This article presents results on the potential of using crystalline flame retardants for thermoset reinforcement. The approach involves introducing reinforcement in thermosetting polymers through low molecular weight crystallizable additives. Thermally induced phase separation (TIPS) and crystallization of desoxyanisoin in diglycidylether of bisphenol-A (DGEBA) epoxy monomer were investigated. Small angle light scattering and polarized optical microscopy were utilized to monitor phase separation and the crystallization of desoxyanisoin in DGEBA at different concentrations. Reaction induced phase separation (RIPS) with polyetheramine was carried out under isothermal and temperature gradient curing conditions. Altering the cure schedule resulted in a rich range of morphologies due to the competition between TIPS and RIPS. During isothermal cure, straight fiber-like anisotropic crystals on a centimeter length scale developed. In contrast, thermal gradients frustrated the crystal growth and resulted in complex and rich morphologies. Desoxyanisoin provided marginal epoxy thermoset reinforcement at 10 vol %. However, the additive did not increase the thermoset flammability retardancy. © 2013 Wiley Periodicals, Inc. *J. Appl. Polym. Sci.* **2014**, *131*, 39853.

KEYWORDS: crystallization; composites; thermosets; fibers; morphology

Received 17 June 2013; accepted 15 August 2013

DOI: 10.1002/app.39853

INTRODUCTION

The incorporation of additives allows polymeric materials to cover a wide range of applications that might otherwise be unattainable. For example, short glass or carbon fibers are commonly introduced to improve stiffness and strength of the material. However, one drawback to this approach is the increase in the process viscosity caused by the fibers.^{1–3} The use of low molecular weight (LMW) crystallizable additives is an alternate strategy to using ridged reinforcements. This approach involves introducing LMW organic crystallizable compounds into a polymer matrix that, at process temperatures, become miscible with polymer or monomer thereby lowering the process viscosity.⁴ Upon cooling or reaction, the LMW compound undergoes temperature induced phase separation (TIPS) and/or reaction induced phase separation (RIPS) and crystallizes, thereby providing unique *in-situ* reinforced composites.

Yoon et al. demonstrated this approach by using a LMW crystallizable additive tetrabromobisphenol A (TBBPA) to provide reinforcement in isotactic polypropylene (iPP). The authors showed that at processing temperatures TBBPA becomes miscible with iPP and reduces viscosity. Upon cooling, TIPS takes place, which results in morphology that improves polymer mechanical properties of iPP.^{5,6} Another example of using this approach was demonstrated by Yordem et al. The authors used a LMW crystallizable additive dimethylsulfone (DMS) to show

that RIPS of DMS in diglycidylether of bisphenol-A (DGEBA) epoxy monomer produced unique composites with distinct reinforcement morphologies.⁷

This study investigates using desoxyanisoin, which is a precursor to making a non-halogenated flame retardant molecule 4,4-bishydroxydeoxybenzoin (BHDB), as a LMW additive for epoxy thermoset. Prior research showed that incorporation of BHDB into the polymer backbone as a replacement for bisphenol-A leads to improved flammability properties.^{8,9} We are interested in investigating whether desoxyanisoin can be used as an additive that will simultaneously improve mechanical and flame retardant properties. It has been shown that LWM organic compounds tend to form fiber-like, dendritic and small sphere-like crystals.¹⁰ This article presents initial results on fiber-like anisotropic desoxyanisoin crystals for thermoset reinforcement as well as frustration of crystal morphology by introducing various thermal gradients.

EXPERIMENTAL

Materials

EponTM 828, a diglycidylether of bisphenol-A (DGEBA), supplied by Resource Resins, was used as an epoxide monomer. The cross-linked networks were formulated by using an aliphatic diamine curing agent (Jeffamine D400, Salt Lake City, UT). Desoxyanisoin (Sigma-Aldrich) was used as the organic crystal in the epoxy network. The chemical structures for the

Table I. Compound Chemical Structure.

Chemical Name	Structure
Desoxyanisoin (Sigma-Aldrich)	
DGEBA (Epon 828 Resource Resins)	
Polyetheramine ($n = 5.6$) (Huntsman D400, Salt Lake City, UT)	

epoxide monomer, the aliphatic diamine and the desoxyanisoin compound are provided in Table I. Toluene (Sigma-Aldrich) was used as the solvent for growing single desoxyanisoin crystals.

Sample Preparation

Temperature Induced Phases Separation (TIPS). Blends of DGEBA with 15, 20, 25, 30, 40, and 50 vol % desoxyanisoin were prepared for performing small angle light scattering (SALS) miscibility and cloud point experiments. To produce a homogeneous solution, desoxyanisoin was dissolved in DGEBA at the minimum necessary temperature. After the desoxyanisoin was completely dissolved, the mixture was allowed to come to room temperature and left for enough time for crystals to grow. It is noted that the crosslinking agent was not added.

Reaction Induced Phase Separation (RIPS). For desoxyanisoin-epoxy thermoset fabrication, desoxyanisoin was dissolved in DGEBA at 80°C. Once a homogeneous solution was obtained, stoichiometric amount of the crosslinking agent was added while the mixture was vigorously stirred. Following the addition of the crosslinking agent, the mixture was poured into 6 by 4 inch plaques and cured for 24 h isothermally at 60°C or with thermal gradient when noted. It is noted that the crosslinking reaction started before desoxyanisoin crystallization.

Characterization

Miscibility and Phase Separation. Crystallization of neat desoxyanisoin and neat desoxyanisoin phase behavior in cured epoxy networks were evaluated under nitrogen with differential scanning calorimetry (DSC) TA Instruments Q200. Two heating and cooling cycles were applied to the samples in the temperature range of -50 to 150°C . With a constant rate of $10^\circ\text{C}/\text{min}$. The data was collected from the first cooling cycle and the second heating cycle. Miscibility and cloud point experiments were carried out with small angle light scattering (SALS). Detailed SALS set up is reported elsewhere.⁷ A sample was placed into the heating stage and as a sample was heated and cooled at $10^\circ\text{C}/\text{min}$, data from scattering image, time, temperature and intensity were recorded simultaneously.

Morphology and Crystal Structure. Polarized Optical Microscopy was conducted with Olympus BX51 and used to examine the size and morphologies of the desoxyanisoin crystals. In

addition, crystal dimensions were evaluated with scanning electron microscopy (SEM), with a Zeiss EVO-50 30kV maximum accelerating voltage. Crystal structures of the samples were analyzed with wide-angle X-Ray scattering (WAXS) Riau S-Max3000 X-Ray instrument with a Cu $K\alpha$ radiation source.

Thermal Properties. Thermal degradation measurements were made with a TA instruments thermogravimetric analysis (TGA) TA Instruments 500. Measurements of the heat-release capacity and total heat released during combustion were made on a pyrolysis-combustion flow calorimeter (PCFC) at $1^\circ\text{C}/\text{s}$. Detailed PCFC set up is reported elsewhere.¹¹

Mechanical Properties. In order to evaluate the young's modulus of desoxyanisoin crystals, single crystals were grown by solvent casting in toluene. Single desoxyanisoin crystals were several centimeters in length and on average 0.2 mm in thickness and 0.6 mm in width. Figure 3 shows the sample width and thickness dimensions of a single desoxyanisoin crystal. Thermo-mechanical analyzer (TMA) TA Instruments 400 with three-point bend test probe was used to measure the Young's modulus of a single desoxyanisoin crystal at room temperature. Reported values were averaged over five measurements.

Tensile properties of the materials were evaluated according to ASTM D638 using Type I specimen on Instron 5800 universal testing machine at room temperature with the crosshead displacement rate of 10 mm/min. Elastic modulus, tensile strength, and elongation at break of both neat epoxy thermosets and desoxyanisoin-epoxy thermosets were measured. Further, extensometer was used for the Poisson's ratio measurements. Reported values were averaged over five measurements.

Dynamic-mechanical characterization of desoxyanisoin-epoxy thermosets was done on dynamic mechanical analyzer (DMA) TA instruments 800 with rectangular bars ($25 \times 5 \times 1 \text{ mm}^3$) in film tension mode. Tests were carried out at 1 Hz as temperature increased from -100°C to 200°C at $3^\circ\text{C}/\text{min}$.

RESULTS AND DISCUSSION

Neat Desoxyanisoin

The crystal structure of desoxyanisoin is monoclinic, with unit cell dimensions of $c = 2.194 \text{ nm}$, $b = 0.5506 \text{ nm}$, and $a = 1.513 \text{ nm}$, and unit cell angles of $\alpha = 90^\circ$, $\beta = 133.9^\circ$, $\gamma =$

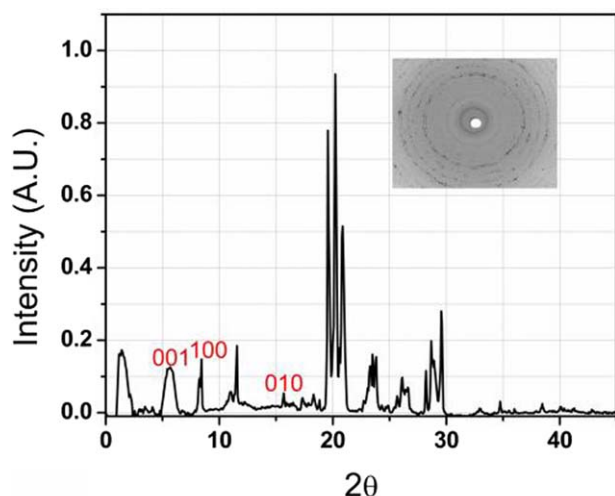


Figure 1. Wide-angle X-ray scattering results for desoxyanisoin crystals. The miller indexes are assigned for the peaks corresponding to crystal growth in *a*, *b*, and *c* directions. [Color figure can be viewed in the online issue, which is available at wileyonlinelibrary.com.]

90°. ¹² Figure 1 presents analysis of the desoxyanisoin crystals used in this study with wide-angle X-Ray scattering (WAXS). As can be seen from Figure 1, the equatorial trace of WAXS diffraction of desoxyanisoin can be resolved into multiple crystal peaks. The dimensions and the angles of the unit cell were used to calculate the *d* spacing corresponding to the crystal growth in *a*, *b*, and *c* directions and Bragg's law was used to calculate the corresponding 2θ locations of crystalline peaks indexed as (100), (010) and (001). Then, the Scherrer equation was used to calculate the apparent crystallite size in *a*, *b*, and *c* directions. The corresponding *d*-spacing, full width half maximum (FWHM), and crystallite sizes are summarized in Table II. The results indicate crystallite size perpendicular to the (100), (010), and (001) planes as 2.4, 44.6, and 36.8 nm, respectively, corresponding to aggregates of small crystallites growing in *a*, *b*, and *c* directions.

The crystallization behavior of neat desoxyanisoin powder was investigated using differential scanning calorimetry (DSC). Many LMW organic compounds form super-cooled glasses and do not recrystallize after melting; such behavior can compromise the mechanical properties of the composite as seen in Yoon et al. work.⁵ In contrast, desoxyanisoin shows a crystallization peak by forming a loop during DSC cooling ramps, as shown in Figure 2(B). The loop in the exotherm forms due to rapid crystallization and associated self-heating resulting from this process.¹³ Rapid crystallization behavior and the ability to recrystallize after melting are important characteristics for in-situ thermoset reinforcement as seen Yordem et al work.⁷

Table II. Apparent Crystallite Size of Desoxyanisoin.

Miller Index	<i>d</i> Spacing (nm)	FWHM (2θ)	Apparent Crystallite Size
001	1.58	10.5	2.44
100	1.09	0.329	36.8
010	0.551	0.021	44.6

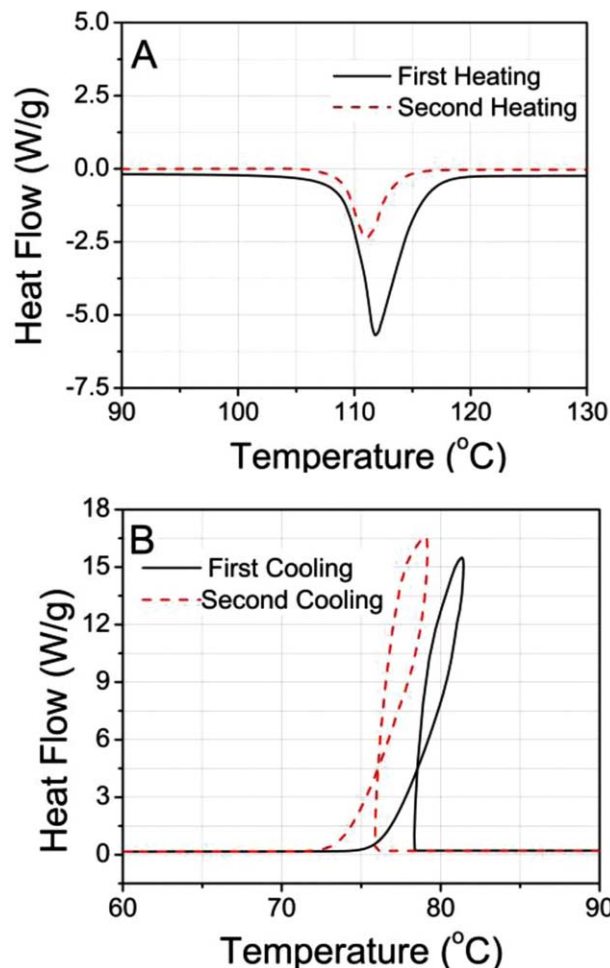


Figure 2. DSC thermograms of desoxyanisoin: (A) heating ramps from 0°C to 150°C, (B) cooling ramps from 150°C to 0°C. [Color figure can be viewed in the online issue, which is available at wileyonlinelibrary.com.]

Figure 3 shows the thickness (A) and the width (B) of a single desoxyanisoin crystal that was used in a TMA flexural test as well as the experimental set up with desoxyanisoin crystal under the probe (C). The ratio of thickness/width is the same as the ratio of the monoclinic unit cell dimensions *b/c* which further confirms that this is a single crystal. The young's modulus of a single desoxyanisoin crystal was calculated to be 65.5 MPa.

Thermally Induced Phase Separation (TIPS) of Desoxyanisoin and DGEBA

TIPS behavior of desoxyanisoin at different volume present in DGEBA was studied theoretically and experimentally in order to insure that in the RIPS experiments described later the diamine curing agent is added while desoxyanisoin and DGEBA are in homogeneous solution. The theoretical melting temperature of desoxyanisoin presents a boundary between its crystalline and liquid state. This temperature was derived by equaling chemical potentials per mole of desoxyanisoin molecule in the crystalline state and in the melt state.¹⁴ In its liquid state, desoxyanisoin is miscible with DGEBA and in its crystalline state desoxyanisoin is completely phase separated and immiscible with DGEBA. The chemical potential of desoxyanisoin in its liquid state was calculated by partial

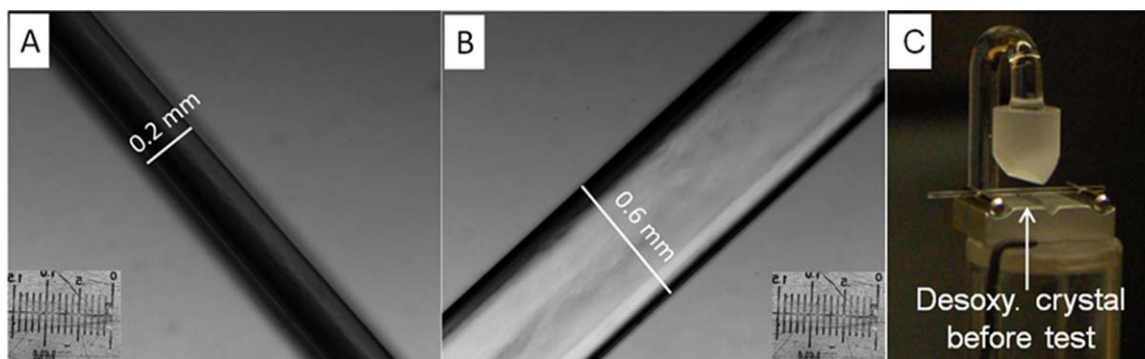


Figure 3. Single Desoxyanisoin Crystal: (A) crystal thickness, (B) crystal width, (C) flexure test set up with desoxyanisoin crystal. [Color figure can be viewed in the online issue, which is available at wileyonlinelibrary.com.]

differentiation of the Flory–Huggins equation for the Gibbs free energy of mixing for two component molecular mixture.¹⁵ The chemical potential of desoxyanisoin in its crystalline state was calculated according to the chemical potential expression for a perfect crystal.¹⁶ By equating the chemical potentials of desoxyanisoin in the liquid state and in the crystalline state, an expression for idealized melting temperature of desoxyanisoin (T_m) was derived in order to estimate equilibrium phase behavior of desoxyanisoin in DGEBA [eq. (1) and solid line in Figure 4].

$$\frac{1}{T_m} = \left\{ 1 + \frac{(\delta_1 - \delta_2)^2 \cdot V_1}{\Delta H_1} (1 - \phi_1)^2 \right\}^{-1} \left\{ \frac{1}{T_m^0} + \frac{R}{\Delta H_1} \cdot \ln \phi_1 \right\} \quad (1)$$

Where δ_1 is the solubility parameter of desoxyanisoin; δ_2 is the solubility parameter of DGEBA, V_1 is the molar volume of desoxyanisoin, ϕ_1 is the volume fraction of desoxyanisoin, and ΔH_1 is the enthalpy of fusion of desoxyanisoin measured in DSC. The solubility parameters and the molar volumes were calculated according to Fedors and Krevelen's approach.^{17–20} This estimation was done in order to predict the temperature at which desoxyanisoin phase separates and precipitates out of the solution with DGEBA.

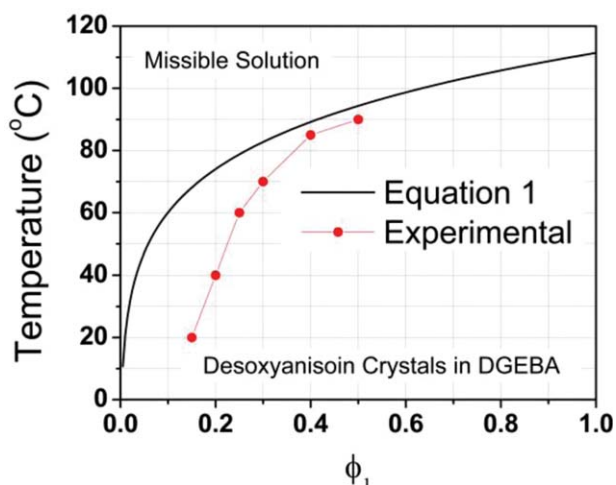


Figure 4. Estimated and experimentally determined equilibrium phase behavior of desoxyanisoin and DGEBA monomer blend. [Color figure can be viewed in the online issue, which is available at wileyonlinelibrary.com.]

In addition to theoretical treatment of TIPS of desoxyanisoin in DGEBA, TIPS was investigated experimentally with small angle light scattering (SALS), dotted line in Figure 4. During the SALS cloud point experiments, transmittance, and real-time information about the evolving crystal morphology are recorded. The transmittance is at its maximum when the solution is clear and desoxyanisoin is completely miscible with DGEBA. As the temperature is decreased, desoxyanisoin phase separates, and transmittance decreases. The transmittance drops to zero, once the morphology is fully developed. Temperature at which the transmittance decreased by 2% from the original value was used as a temperature at which phase separation between desoxyanisoin and DGEBA takes place.

As can be seen from Figure 4, there is a large discrepancy between the estimated equilibrium phase behavior and the experimental measurements. This occurs because the estimated phase behavior is based on the thermodynamics that does not consider kinetic effects. However, as desoxyanisoin concentration and the temperature are decreased, kinetic effects become dominant and there is a deviation from the estimated behavior. Therefore, for lower volume fractions of desoxyanisoin in DGEBA, the solution has to be brought to lower temperatures in order for desoxyanisoin crystals to form. The theoretical and experimental analysis of TIPS of desoxyanisoin in DGEBA was carried out to insure that the cross-linking reaction between DGEBA and diamine curing agent started before desoxyanisoin crystallization. Thus, we could insure that for desoxyanisoin–epoxy thermosets the RIPS always started before TIPS.

Desoxyanisoin–Epoxy Thermosets

Desoxyanisoin–epoxy thermosets were fabricated by curing a desoxyanisoin/DGEBA mixture with polyetheramine cross-linking agent. Altering isothermal cure schedule resulted in rich range of crystal morphologies. Various morphologies are formed due to the competition between reaction induced phase separation (RIPS) and temperature induced phase separation (TIPS) of desoxyanisoin and the epoxy matrix. As an example, when the cross-linking agent is added at high temperatures ($>80^\circ\text{C}$), RIPS proceeds rapidly and only small crystallites can grow [Figure 5(A)]. In contrast, when the cross-linking agent is added at lower temperature ($<70^\circ\text{C}$), TIPS is dominant. At dominating TIPS conditions, *in-situ* large, needle like, highly anisotropic crystal

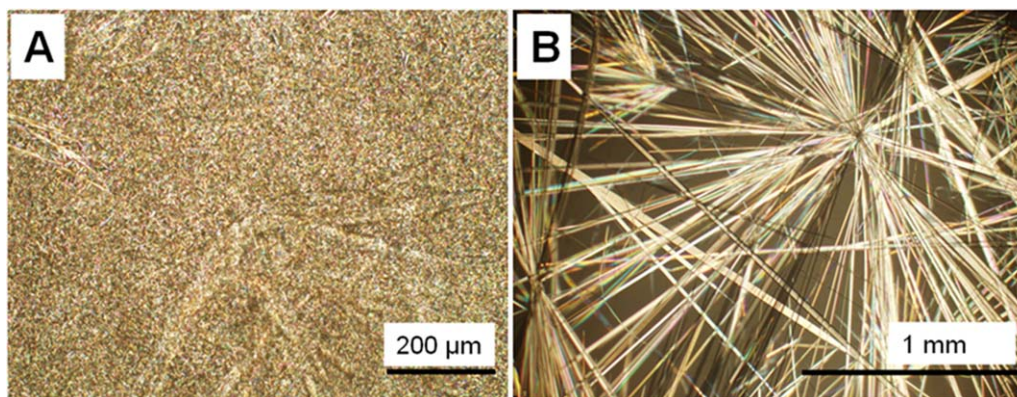


Figure 5. Micrographs of 10 vol % desoxyanisoin composite isothermally cured at different cure schedules: (A) the cross-linking agent is added at high temperatures ($>80^{\circ}\text{C}$) and cured at 80°C ; (B) the cross-linking agent is added at lower temperature ($<60^{\circ}\text{C}$) and cured at 60°C . [Color figure can be viewed in the online issue, which is available at wileyonlinelibrary.com.]

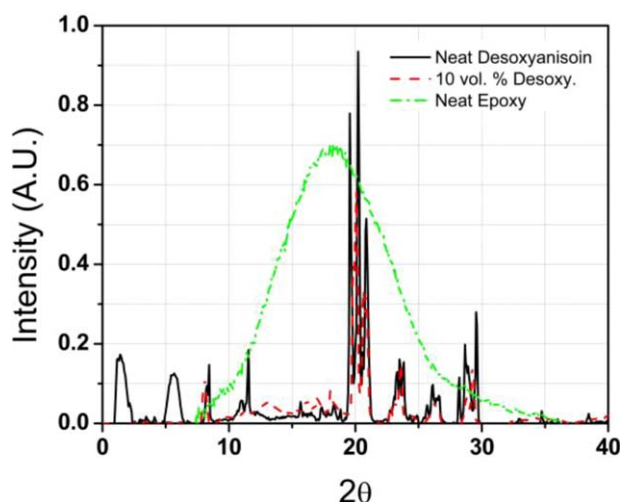


Figure 6. Wide-angle X-ray scattering results for desoxyanisoin–thermoset composite. [Color figure can be viewed in the online issue, which is available at wileyonlinelibrary.com.]

structures grow quiescently, with some needles extending on centimeter scale at appropriate experimental design [Figure 5(B)].

Wide angle X-ray scattering (WAXS) was used to investigate the structure of desoxyanisoin crystals in the epoxy composite. Figure 6 shows that desoxyanisoin crystals retain their monoclinic structure in the cured epoxy matrix. This result was confirmed with SEM images. Figure 7(A) shows an image of a hole remaining after a fiber crystal was pulled from the resin. The aspect ratio of the sides of the hole is within the range of the aspect ratio between sides b and c of the desoxyanisoin crystal unit cell. The angles are consistent with the unit cell angles between sides b and c as well. The geometry of b – c plane further indicates poor adhesion between desoxyanisoin crystals and the epoxy matrix. Similarly, Figure 7(B) shows the a – c plane of a single crystal with a and c sides at 133.9° to each other.

Figure 8 shows desoxyanisoin crystallization behavior in an epoxy thermoset investigated with DSC. The absence of the crystallization peak in the cooling ramps and shift to lower melting temperature and lower enthalpy of melting in comparison to neat desoxyanisoin can be explained by slow crystallization kinetics. Further, during the cooling cycle there is a shift to lower glass transition temperatures for desoxyanisoin containing composites. This suggests that, due to the extremely slow kinetics of desoxyanisoin crystallization, some of the desoxyanisoin remains trapped within the epoxy.

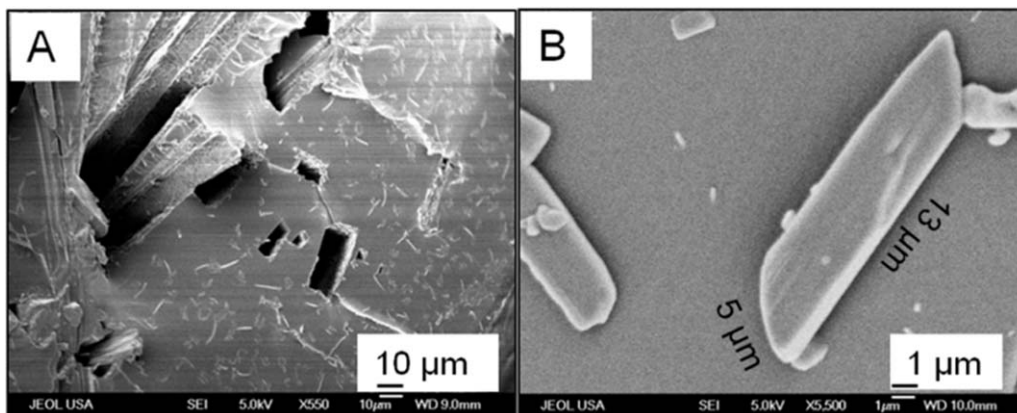


Figure 7. SEM images of reinforcement morphology of desoxyanisoin crystals in thermoset composite: (A) reinforcement pull out and (B) a – c plane of a single desoxyanisoin crystal.

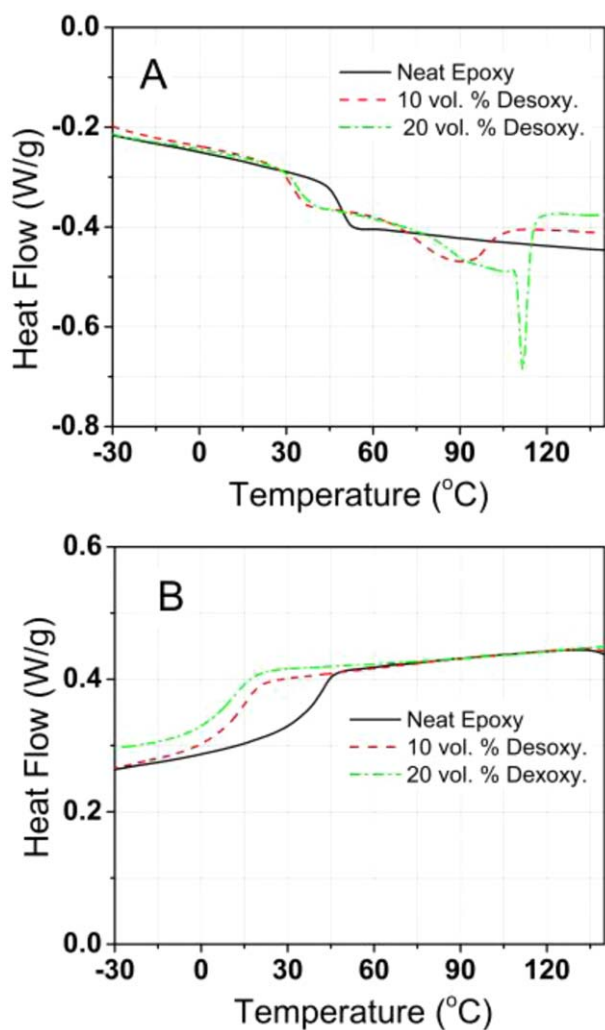


Figure 8. DSC thermograms for 10 and 20 vol % desoxyanisoin–thermoset composite and pure thermoset as control at 10°C/min: (A) heating ramps and (B) cooling ramps. [Color figure can be viewed in the online issue, which is available at wileyonlinelibrary.com.]

Mechanical Properties of Desoxyanisoin–Epoxy Thermosets

Dynamic Mechanical Analysis (DMA) was performed to investigate if desoxyanisoin crystals provided any reinforcement. Desoxyanisoin provided some reinforcement in the glassy state, as observed in higher storage modulus shown in Figure 9(A). However, DMA results showed no reinforcement in the rubbery state. Similarly to DSC results, glass transition temperature for the desoxyanisoin containing composites measured with DMA was lower than for the unfilled cross-linked epoxy matrix suggesting that some of the additive remained miscible with the epoxy [Figure 9(B)].

Table III presents the tensile test results on desoxyanisoin–epoxy thermosets. The Young's modulus and Poisson's ratio of 10 vol %

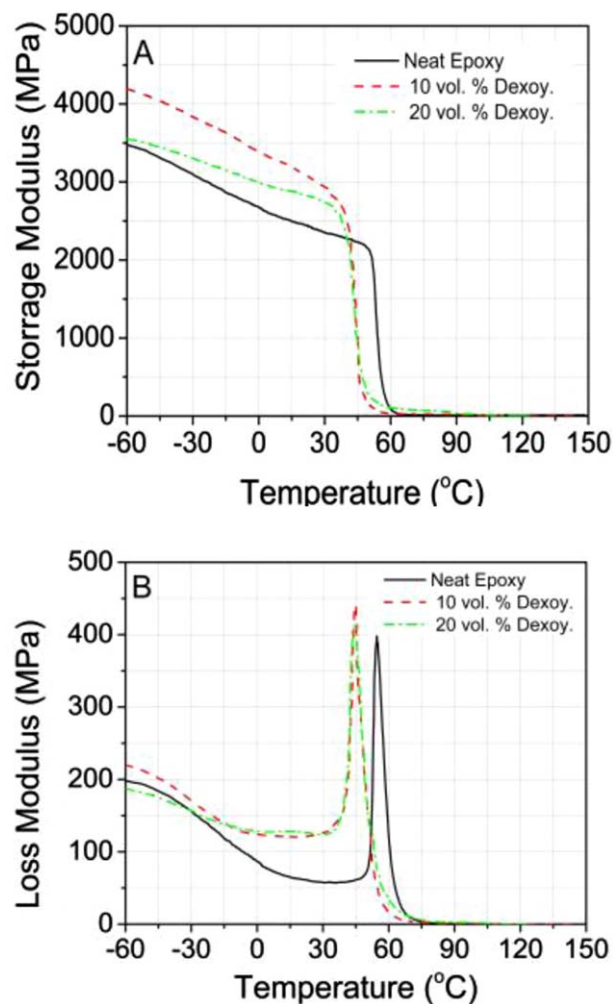


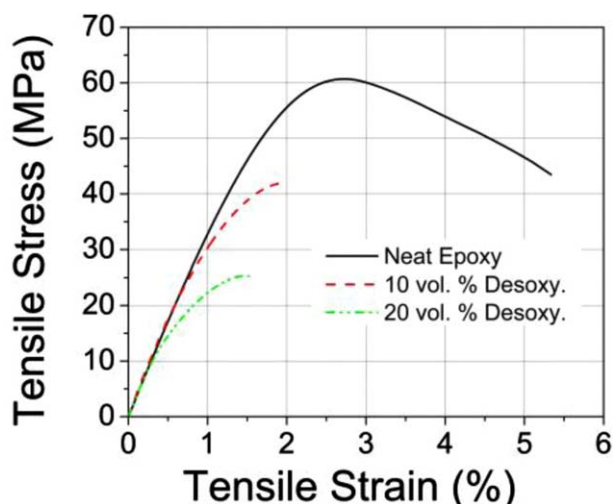
Figure 9. DMA result measured at 1 Hz, 3°C/min heating rate: (A) storage modulus and (B) loss modulus. [Color figure can be viewed in the online issue, which is available at wileyonlinelibrary.com.]

desoxyanisoin composite increased in comparison to neat epoxy. However, the tensile yield strength and the elongation at break decreased with the addition of desoxyanisoin at all concentrations as can be seen in Figure 10. The theoretical composite moduli were calculated according to Christensen's model for finite length fibers in the composite matrix [eq. (2)].²¹ The Lamé's Constants (μ and λ), were calculated from measured Young's Modulus and Poisson's Ratio for neat epoxy and from measured Young's Modulus and estimated Poisson's ratio of 0.4 for desoxyanisoin crystal. Note that when a value for the Poisson's ratio in the range between 0.3–0.49 is used for crystal the composite moduli values deviated by 0.1–0.4%. Therefore, the moduli are reported using the estimated Poisson's ratio value of 0.4 (Figure 11).

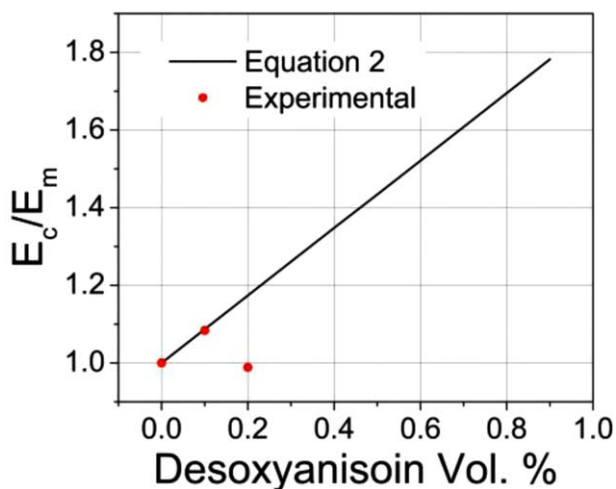
$$\frac{E_c}{E_m} = 1 + c \frac{\frac{\Delta\mu}{2(1-\nu_m)} (3\Delta\lambda + 2\Delta\mu) + \frac{E_m(1-2\nu_m)}{2(1+\nu_m)} \Delta\lambda + \frac{E_m(1+2\nu_m^2)}{(1+\nu_m)(1-2\nu_m)} \Delta\mu}{\Delta\mu(3\Delta\lambda + 2\Delta\mu) \left(\frac{1+\nu_m}{1-\nu_m} \right) k^2 \left[\ln \frac{2}{k} - \frac{5-4\nu_m}{4(1-\nu_m)} \right] + \frac{E_m}{2(1-\nu_m)} (\Delta\lambda + \Delta\mu) + \mu_m(3\lambda_m + 2\mu_m)} \quad (2)$$

Table III. Tensile Test Results of Desoxyanisoin-Epoxy Composites.

	Young's Modulus (MPa)	Poisson's Ratio	Yield Strength (MPa)	Elongation at Break (mm/mm)
Neat Epoxy	35	0.30	60	2.7
10 vol % Desoxyanisoin	38	0.32	42	1.93
20 vol % Desoxyanisoin	35	0.30	25	1.52

**Figure 10.** Tensile test curves for neat epoxy, 20 and 10 vol % desoxyanisoin composites. [Color figure can be viewed in the online issue, which is available at wileyonlinelibrary.com.]

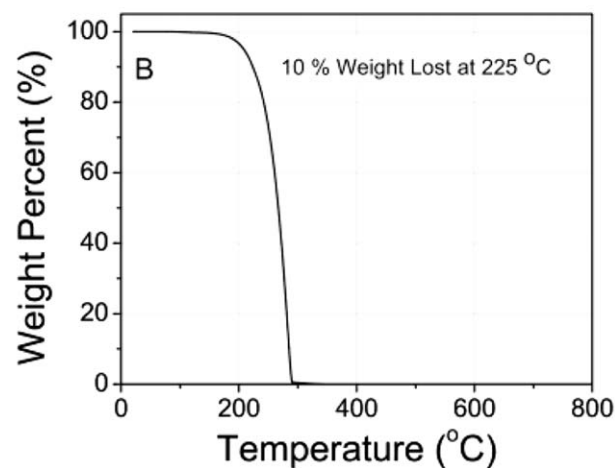
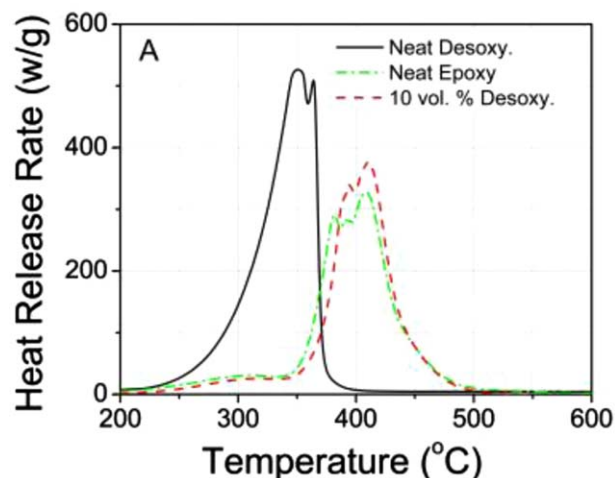
Where E_c is the young's modulus of the composite; E_m is the young's modulus of the epoxy matrix; c is the vol % of desoxyanisoin; $\Delta\mu$ is the difference between the shear moduli of the

**Figure 11.** Theoretical and experimntal moduli dependency on desoxyanisoin concentration. [Color figure can be viewed in the online issue, which is available at wileyonlinelibrary.com.]**Table IV.** Compound Flammability Properties Measured by PCFC.

	Neat Desoxyanisoin	Neat Epoxy	10 vol % Desoxyanisoin
Heat release capacity HRC (J/(g K))	590	491	530
Total heat released (kJ/g)	29.8	23.3	24.4
PCFC char yield (%)	1.2	7.1	6.6

desoxyanisoin fiber (μ_f) and of the epoxy matrix (μ_m); $\Delta\lambda$ is the difference between the Lamé's first parameter of the desoxyanisoin fiber (λ_f) and the Lamé's first parameter of the epoxy matrix (λ_m); k is the width to length aspect ratio of desoxyanisoin crystal and ν_m is Poisson's ratio of the epoxy matrix.

As can be seen from Figure 11, the measured young's modulus and the theoretical young's modulus for 10 vol % desoxyanisoin composite are in agreement. This result indicates that desoxyanisoin provides some reinforcement to the epoxy matrix at lower concentrations and that the Christensen model is accurate

**Figure 12.** (A) PCFC heat release rate versus temperature; (B) TGA analysis for neat desoxyanisoin. [Color figure can be viewed in the online issue, which is available at wileyonlinelibrary.com.]

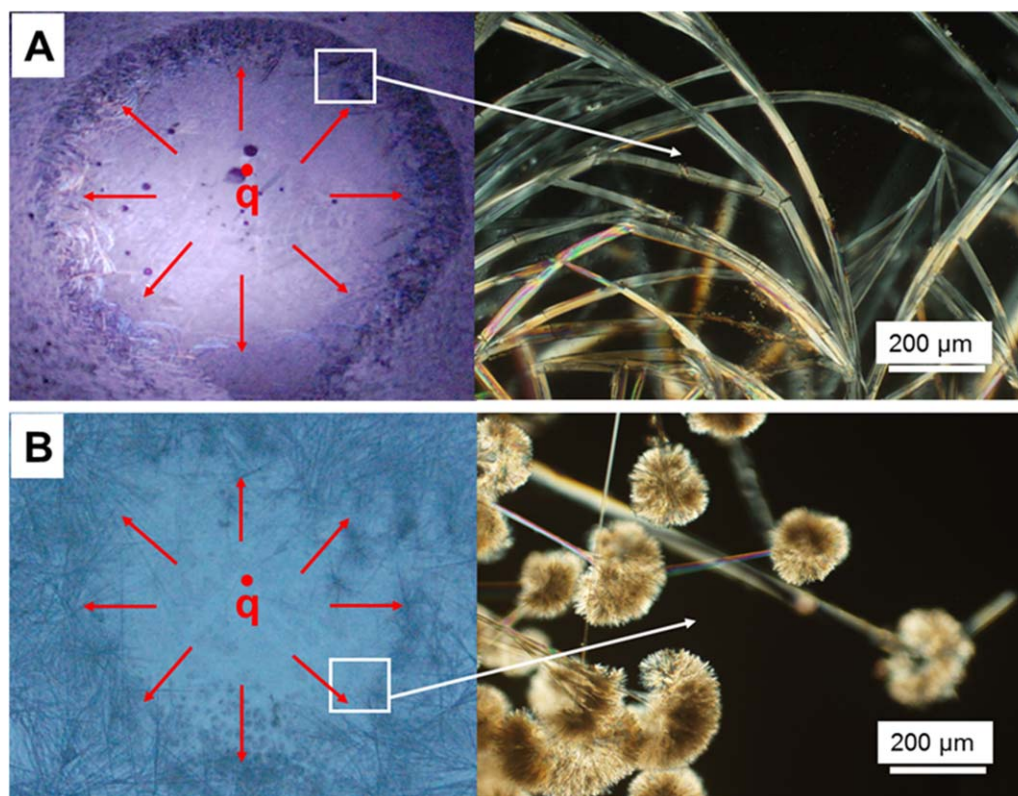


Figure 13. Micrographs of frustrated desoxyanisoin crystal growth with thermal gradients: (A) discontinuity in crystal growth and cracking of crystals, which appears as curvature; (B) discontinuity in crystal, which appears as a dendritic structure with a number of crystals growing in close proximity. [Color figure can be viewed in the online issue, which is available at wileyonlinelibrary.com.]

at lower concentrations. However, at higher concentrations of (20% vol), the measured modulus is significantly lower than the predicted value. This finding suggests the presence of a critical concentration of desoxyanisoin above which it ceases to improve the modulus of the epoxy thermoset. It is evident from the shift in the glass transition to lower temperatures seen in DMA that some of desoxyanisoin stays miscible in the epoxy matrix, therefore leading to the deterioration in the mechanical properties and the deviation from the theoretical predictions. A detailed study across a wide range of concentrations of desoxyanisoin in the epoxy matrix is required for further understanding of the concentration threshold effect on the mechanical properties of the composite.

Flammability

Pyrolysis-combustion flow calorimeter (PCFC) analysis did not show an improvement in the epoxy composite flammability characteristics with the addition of desoxyanisoin; the important flame retardant properties are summarized in Table IV and Figure 12(A). Desoxyanisoin has a high vapor pressure and a low boiling point. As can be seen from Figure 12(B), the desoxyanisoin starts to boil off and loses 10% of its weight as early as 225°C. Thus, the desoxyanisoin actually boils off from the epoxy composite before the epoxy matrix reaches its degradation temperature rendering no improvement in flame retardant properties. However, modifying the desoxyanisoin molecular structure to stabilize in the epoxy as it reaches its degradation temperature might result in more favorable results. Such modi-

fications can be done by either increasing the molecular weight of the desoxyanisoin molecule or by putting reactive groups on the desoxyanisoin molecule, thereby enabling it to become part of the epoxy network.

Frustrated Reinforcement Morphologies with Thermal Gradients

After an initial understanding of isothermal phase separation of desoxyanisoin in a cross-linked epoxy matrix, various thermal gradients were used to investigate how these thermal gradients would alter crystal morphology. Figure 13 shows examples of crystal morphologies formed from a radially symmetric thermal gradient. No crystals are formed immediately near the center (location of the heat source). In this region, the cross-linking reaction happens so rapidly that there is no time for the crystals to grow and desoxyanisoin diffuses away from this region. At some critical radial distance, a transitional region is observed. Figure 13(A) illustrates discontinuity in crystal growth and local cracking of crystals, which appears as curvature. Similarly, Figure 13(B) illustrates discontinuity in crystal growth caused by a different temperature gradient, which appears as a dendritic structure with a number of crystals growing in close proximity. Figure 14 illustrates yet another central temperature gradient applied to a thicker film and shows the richness of morphologies that can be obtained. Further, far away from the central heat source when the curing condition is almost isothermal, dramatic differences in morphology are observed again and fiber-like crystal growth is present.

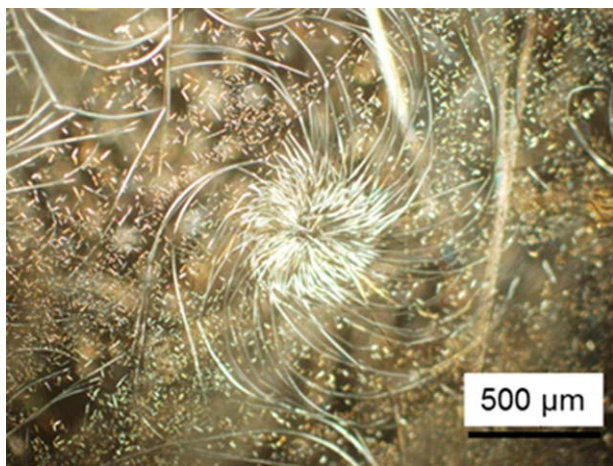


Figure 14. Micrograph of frustrated desoxyanisoin crystal growth in thermoset composite. [Color figure can be viewed in the online issue, which is available at wileyonlinelibrary.com.]

The control of crystal morphology is important for many fields and applications, such as in the fabrication of nano-scale devices, in the uptake of lipophilic vitamins and drugs, and in non-linear optics (NLO).^{22,23} Our results are consistent with work by Lofgren et al. who showed that with a substantial degree of supercooling, curved, and branched crystal morphologies can be produced.²⁴ Similarly, Cheng et al. have reported that the temperature and the solute concentration distribution determine the crystal shape.²⁵ Further, when the curvature of the crystal is present, it can be shaped by either the temperature or the concentration gradient.^{26,27}

CONCLUSION

A low molecular weight additive, desoxyanisoin, was investigated both as a potential *in situ* reinforcement agent and as a flame retardant. In addition, this study focused on crystal growth morphology under isothermal condition and various thermal gradients, in order to frustrate crystal growth and alter the reinforcement morphology. Desoxyanisoin is a crystallizable compound that is miscible in epoxy monomer at elevated temperatures, but undergoes TIPS and crystallizes on its own. However, the kinetics is slow. During RIPS with diamine curing agent desoxyanisoin undergoes phase separation under quiescent conditions. Desoxyanisoin provides *in situ* highly anisotropic growth of straight fiber-like crystals during the isothermal cure of epoxy thermosets. Crystals extend on the centimeter length scale, when suitable polymerization conditions are met. Sharp temperature gradient curing condition resulted in complex morphologies such as curved or branched crystals. The variety of morphologies is formed due to the interplay between the curing reaction of epoxy networks and TIPS/crystallization of desoxyanisoin. Utility of this LMW crystallizable additive as a flame retardant is limited. Due to its low boiling point and high vapor pressure, it sublimes out of the composite prior to epoxy matrix reaching decomposition temperature. Further chemical modification of the desoxyanisoin molecule is necessary in order to utilize it as a flame retardant. Desoxyanisoin provided some thermoset rein-

forcement at 10 vol %, but not at higher concentrations. As can be seen from DSC and DMA analysis, there is a shift in the glass transition to lower temperature when desoxyanisoin is incorporated into the epoxy-thermoset composite. This suggests that some of desoxyanisoin stays miscible in the epoxy matrix, which can lead to the deterioration in the mechanical properties especially at higher concentrations.

REFERENCES

- Joshi, M.; Maiti, S. N.; Misra, A. *Polymer* **1994**, *17*, 3679.
- Kalaprasad, G.; Mathew, G.; Pavithran, C.; Thomas, S. *J. Appl. Polym. Sci.* **2003**, *2*, 432.
- Yordem, O. S.; Lesser, A. J. *SPE-ANTEC Tech. Papers*; **2010**.
- Lesser, A. J.; Clzi, K.; Junk, M. *Polym. Eng. Sci.* **2007**, *47*, 1569.
- Yoon, J.; McCarthy, T. J.; Lesser, A. J. *J. Appl. Polym. Sci.* **2009**, *113*, 3564.
- Lesser, A. J.; McCarthy, T. J.; Yoon, J.; Yordem, O. S. Reinforced Polymeric Materials, Methods of Manufacture Thereof and Articles Comprising the Same. University of Massachusetts, Amherst; **2008**.
- Yordem, O. S.; Lesser, A. J. *J. Polym. Sci. Part B Polym. Phys.* **2010**, *48*, 840.
- Ranganathan, T.; Beaulieu, M.; Zilberman, J.; Smith, D. K.; Westmoreland, R. P.; Farris, J. R.; Coughlin, E. B.; Emrick, T. *Polym. Degrad. Stab.* **2008**, *93*, 1059.
- Ellzey, A. K.; Zilberman, J. R.; Coughlin, E. B.; Farris, J. R.; Emrick, T. *Macromolecules* **2006**, *39*, 3553.
- Narkis, M.; Siegmann, A.; Puterman, M.; Di Benedetto, A. *T. J. Polym. Sci.: Polym. Phys. Ed.* **1979**, *17*, 25.
- Lyon, R. E.; Walters, R. N. *J. Anal. Appl. Pyrolysis* **2004**, *71*, 27.
- DiMarco, J. The Polytechnic University, Physics Department, Brooklyn, New York, ICDD Grant-in-Aid; **1990**.
- Anestiev, L.; Malakhov, D. J. *Noncryst. Solids* **2006**, *352*, 3350.
- Young, R. J.; Lovell, P. A. Introduction to Polymer, 2nd ed.; Chapman & Hall: London; **1991**.
- Flory, P. J. Principles of Polymer Chemistry; Cornell University Press: Ithaca, NY; **1953**.
- Strobl, G. The Physics of Polymers, 3rd ed.; Springer: Berlin; **2007**.
- Fedors, R. F. *Polym. Eng. Sci.* **1974**, *14*, 147.
- Houge, O. A.; Watson, M. K.; Ragatz, R. A. *Chem. Process Principles Parts I and II*; **1964**.
- Perry, R. H.; Chilton, C. H. Chemical Engineer's Handbook, 5th ed.; Cecil H. Chilton; **1973**.
- Hoflyzer, D. W.; Krevelen, V. Handbook of Polymer-Liquid Interaction Parameters and Solubility Parameters: Properties of Polymer Relations with Chemical Structure. Barton, A. F. M., editor; CRC Press: Boca Raton, FL; **1990**.
- Christensen, R. M. Mechanics of Composite Materials; Dover Publishers; **2005**.

22. Karthaus, O.; Nagata, S.; Kiyono, Y.; Ito, S.; Miyasaka, H. *Colloids Surf A: Physicochem. Eng. Aspect.* **2008**, *313*, 571.
23. Zhang, D. E.; Pan, D. X.; Zhu, H.; Li, S. Z.; Xu, G. Y.; Zhang, B. X.; Ying, L. A.; Tong, W. Z. *Nanoscale Res. Lett.* **2008**, *3*, 284.
24. Lofgren, E. G.; Donaldson, H. C. *Contrib. Mineral. Petrol.* **1975**, *49*, 309.
25. Cheng, Z. D. S.; Lotz, B. *Phil. Trans. R. Soc. Lond. A* **2003**, *361*, 517.
26. Rathi, P.; Park, S. J.; Kyu, T. *J. Chem. Phys.* **2009**, *130*, 174904.
27. Park, S. J.; Rathi, P.; Kyu, T. *Phys. Rev. E* **2007**, *75*, 051804.